JOURNAL OF AEROSPACE SOCIETY MALAYSIA

ARTICLE

EFFECT OF AEROFOIL THICKNESS ON THE WIND TURBINE BLADE: CASE STUDY OF FFA-W3-270 AND FFA-W3-240 AEROFOIL

Nur Natasha Ayuni Nazri [1,*] and Shabudin Mat [1]

1. UTM Aerolab, Institute for Vehicle System & Engineering (IVeSE), Universiti Teknologi Malaysia, Malaysia.

*Correspondence: nurnatashaayuni@gmail.com

Abstract: Due to the climate change nowadays, there are a lot of alternative ways to convert renewable energy to generate electricity and the wind energy is one of them. Reynold's numbers of 0.8×10^6 and 1.0×10^6 are compared in this study to see their effects on the FFA-W3-270 and FFA-W3-240 aerofoil models. The dimension of the FFA-W3-240 type is 120 mm thick, with a chord of 500 mm and a span of 800 mm. In contrast, the FFA-W3-270 type has 128 mm maximum thickness, 500 mm chord and a span of 750 mm. Investigation of the lift force, drag force, pitching moment and pressure distributions on these two aerofoil models is done in a wind tunnel test using UTM LST Wind Tunnel, which has dimensions of 1.5 m x 2 m x 5.8 m. The wind tunnel experiments are carried out at 25 m/s and 31.2 m/s wind stream velocity and angle of attack ranging from -4 ° to 18 ° with an increment of 2°. From the experimental results, it is observed that the pressure coefficient on the upper surface of the FFA-W3-240 has a significant change in comparison to that for the FFA-W3-270. When the adverse pressure gradient increases, it causes earlier separation for thinner aerofoil. In contrast, it causes separation delay for the thick aerofoil. From this, it shows that FFA-W3-270 has better aerodynamic performance. For FFA-W3-240, at Reynold's number 1.0×10^6, stall occurs at 14° with maximum lift coefficient of 1.26. However, for FFA-W3-270, stall does not occur up until 18°. Besides, for FFA-W3-240, increasing the Reynold's number will increase the drag coefficient at stall point by over 5.48%. For both models, the pitching moment coefficient remains relatively constant over the considered range of angles of attack due the moment being calculated at the aerodynamic center of the aerofoil, which is estimated to be at the quarter-chord location from the leading edge.

Keywords: aerofoil; separation; angle of attack; aerodynamic performance; stall

1. Introduction

Utilizing wind energy typically has a lower environmental impact than using other energy sources. Most buildings now use small-sized wind turbines, especially industrial buildings. The function of this wind turbine is to convert kinetic energy from the rotation of the turbine that is caused by the passing wind into mechanical energy and subsequently, it will be converted into electrical energy. Wind turbines can be divided into two primary categories: horizontal-axis turbines (HAWT) and vertical-axis turbines (VAWT) [1]-[2]. In general, the aerodynamic issues faced by wind turbine operations are mostly caused by adverse pressure gradient, which causes flow separation. The capacity to lessen, regulate or postpone the flow separation will significantly improve an airfoil's aerodynamic performance and consequently will help boost the efficiency of a general turbine [3]. In a recent study, several methods to improve the performance of horizontal wind turbine blades are investigated, which is focused on utilizing multiple airfoil sections and fence [4]. Based on the findings, it has been suggested that these enhancements can lead to improved efficiency and performance of horizontal wind turbines.

For the presented study in this paper, a specialized FFA aerofoil model is used. Among others, this aerofoil design has been developed for the purpose of overcoming the weakness of high drag and low maximum lift coefficient, C_{Lmax} that many thick airfoils commonly exhibit with rough leading [5]. In the previous studies, conducted numerical analysis on the effect of changing thickness to the aerodynamic performance of the aerofoil has demonstrated that increasing the aerofoil thickness will lead to increase in drag coefficient and maximum lift [6]-[7]. Moreover, an analysis on the aerodynamic characteristics of the FFA-W3-270 aerofoil has found that the maximum suction peak value at the leading edge on the suction side varies dramatically when the angle of attack increases, even though the value on the bottom surface does not [8]. This means that, when the Reynolds number rises, the maximum lift will increase, the drag coefficient will decrease and the stall condition will occur at lower angle of attack.

While previous studies have shown that the thickness of the aerofoil has significantly affected the wing's aerodynamic properties, it should be noted that most of these earlier studies used the simulation analysis methods, with only very few involved the experimental trials. Because of this, there is a lack of experimental data for comparison purposes. More specifically, the data for the FFA aerofoil is not well-documented. This study is addressing this identified gap of information.

2. Methodology

In this research, two types of FFA-W3 aerofoil are tested: FFA-W3-240 and FFA-W3-270. These two aerofoil are shown in Figure 1 while the experimental setup for the wind tunnel testing are tabulated in Table 1. Both aerofoil models are tested in the wind tunnel for varied angles of attack between -4° and 18° with 2° increment under two settings of Reynolds' number: 0.8×10^6 and also 1.0×10^6. The LabVIEW application software is used for data acquisition utilizing the computer data logger.

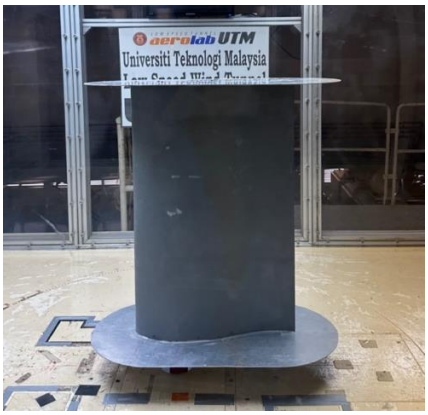

(a) FFA-W3-270 aerofoil

(b) FFA-W3-240 aerofoil

Figure 1: Test models used in this study

Table 1: Experimental setup for the wind tunnel testing

Aerofoil Model	Pressure Taps	Model Size
FFA-W3-270	30 (17 on the upper surface and 13 on the lower surface)	Total span: 750 mm Chord: 500 mm Maximum thickness: 135 mm
FFA-W3-240	36 (21 on the upper surface and 15 on the lower surface)	Total span: 800 mm Chord: 500 mm Maximum thickness: 120 mm

From the experiments, the main results that will be measured are the surface pressure distribution, aerodynamic forces and moments. The FKPS 30DP electronic pressure scanner is used to monitor the surface pressure and an external balance is used to measure the aerodynamic forces and moments. The technical drawing for the FFA-W3-270 model and the illustration on how the model is set up inside the wind tunnel are shown in Figure 2 and Figure 3, respectively.

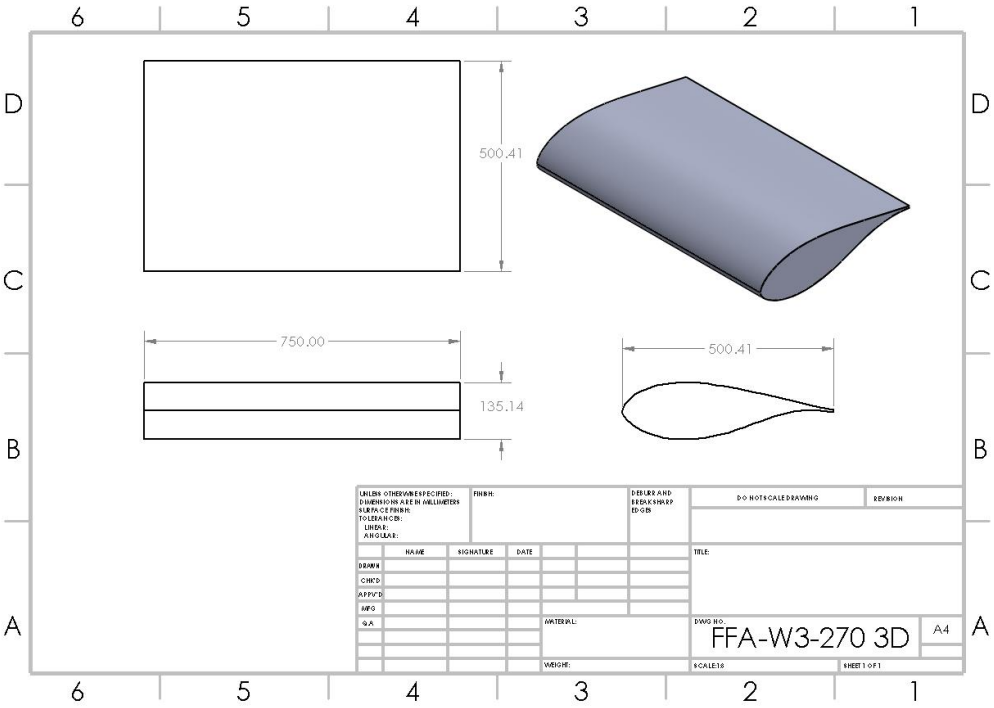

Figure 2: Technical drawing of FFA-W3-270 aerofoil

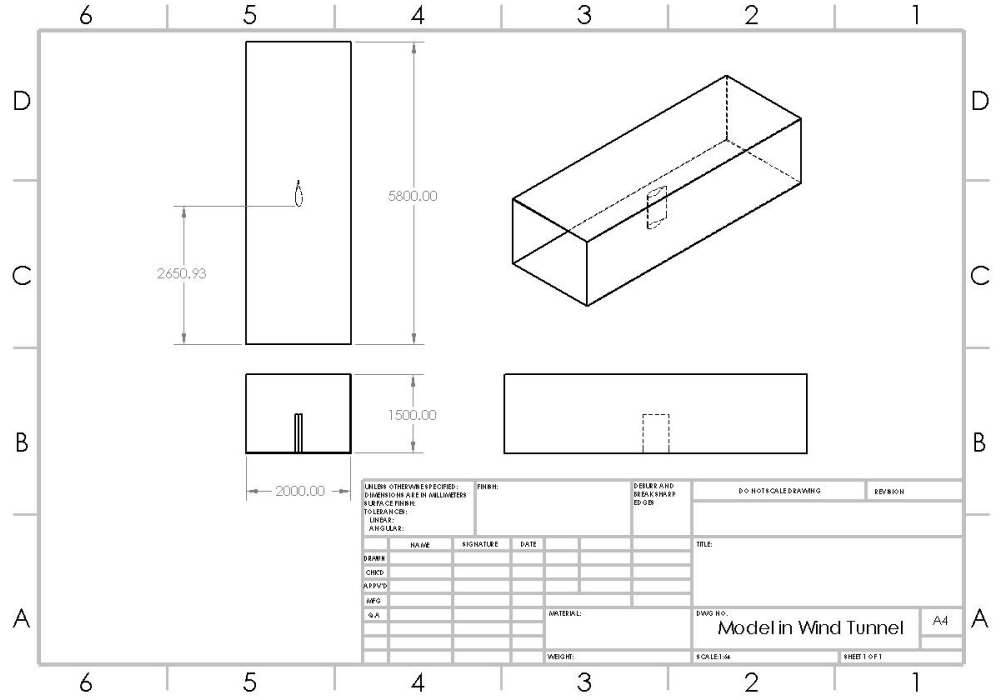

Figure 3: Orientation of the test model in wind tunnel during testing

Figure 4 shows the overall flowchart for the data collection. The data are collected from the wind tunnel testing include lift coefficient (C_L), drag coefficient (C_D), pitching moment coefficient (C_M) and surface pressure of location (X/C) of the aerofoil's pressure coefficient (C_P).

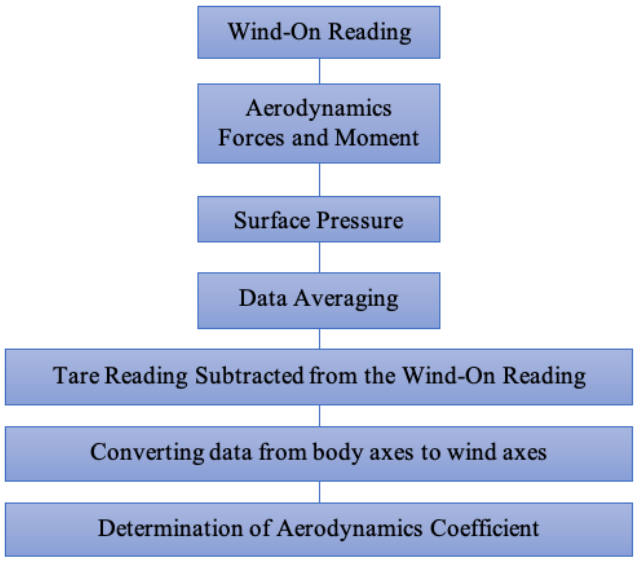

Figure 4: Overall flowchart of data collection and analysis process in this study

3. Results and Discussion

As depicted in Figure 5, for both aerofoil models at angle of attack of -4°, the pressure coefficient, C_P of the lower surface is lower than that of the upper surface at the leading edge. Moving down to the trailing edge, at X/C = 0.612, the C_P value for both upper and lower surfaces intersects, after which C_P for the lower surface increases gradually. This shows that the pressure for lower surface at the leading edge is lower than the freestream pressure. Furthermore, as shown in Figure 6 for both aerofoil models, at angle of attack of 0°, C_P value for the upper surface is lower than that for the lower surface. With further increase in angle of attack, for example as indicated by Figure 7 for angle of attack of 10°, the maximum suction peak value at the leading edge on the suction side significantly changes whereas the value for the lower surface does not change much. It can be observed that C_P on the upper surface of the FFA-W3-240 aerofoil has a big significant change compared to that for the FFA-W3-270 aerofoil.

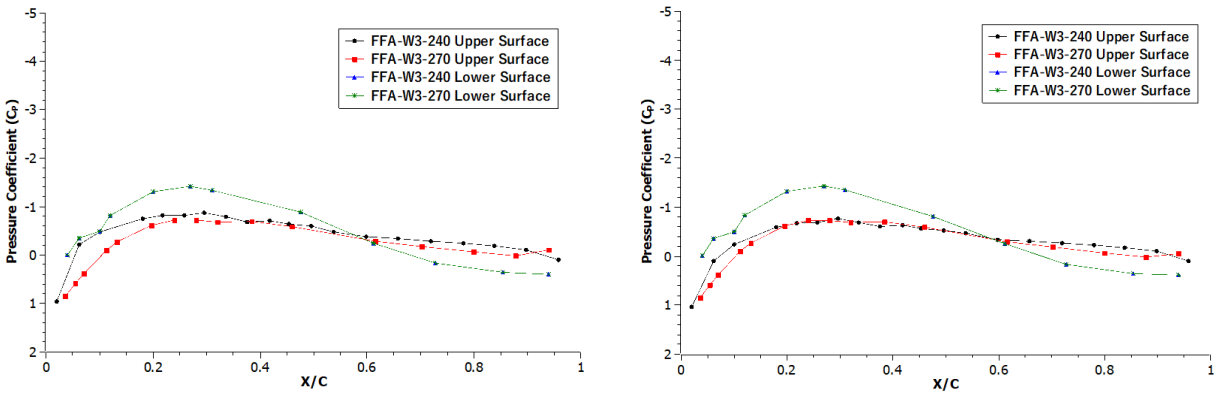

(a) Re = 0.8 × 10^6 (b) Re = 1.0 × 10^6

Figure 5: *Cp* versus X/C at angle of attack of -4°

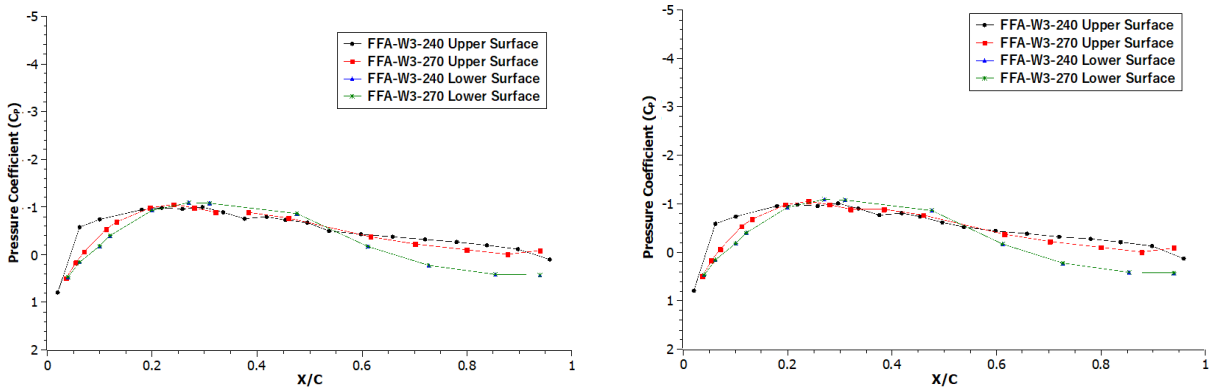

(a) Re = 0.8 × 10^6 (b) Re = 1.0 × 10^6

Figure 6: *Cp* versus *X*/*C* at angle of attack of 0°

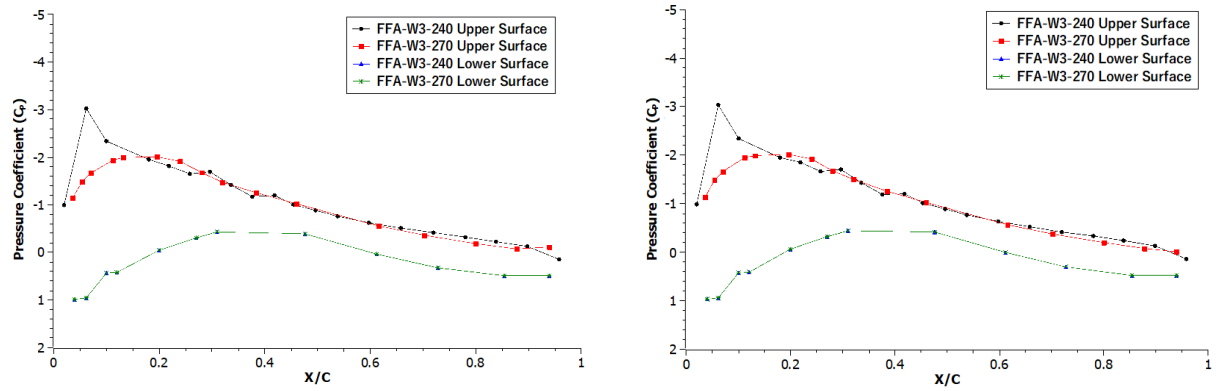

(a) Re = 0.8 × 10^6 (b) Re = 1.0 × 10^6

Figure 7: *Cp* versus *X*/*C* at angle of attack of 10°

The full separation starts to occur after the stall angle. By comparing the plot for angle of attack of 16° in Figure 8 and angle of attack of 18° in Figure 9, the separation point can be seen to start moving forward. For instance, this situation can be observed for the upper surface of the FFA-W3-270 aerofoil in Figure 8 and Figure 9 whereby as the angle of attack increases, the maximum C_P value starts to move towards leading edge. This observation is in line with findings from other studies that, as the angle of attack increases, the separation points progressively shift towards the leading edge [9]-[10].

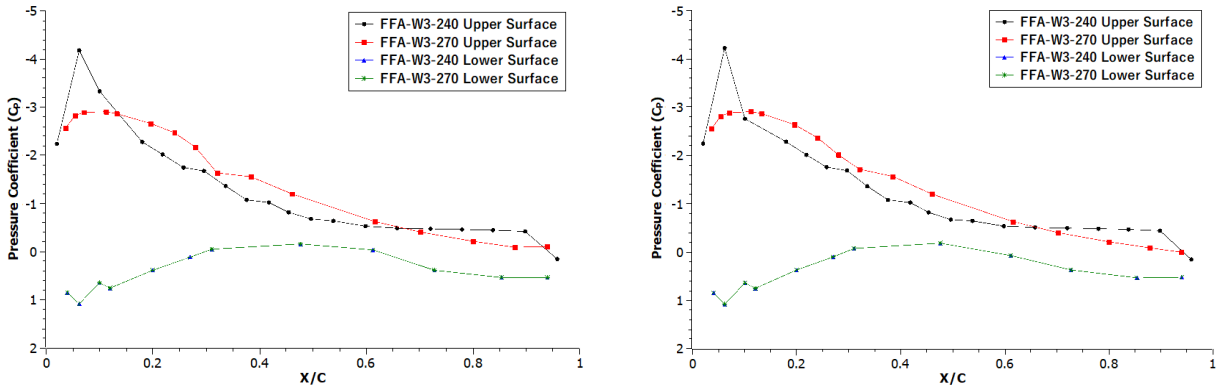

(a) Re = 0.8 × 10^6 (b) Re = 1.0 × 10^6

Figure 8: *Cp* versus *X*/*C* at angle of attack of 16°

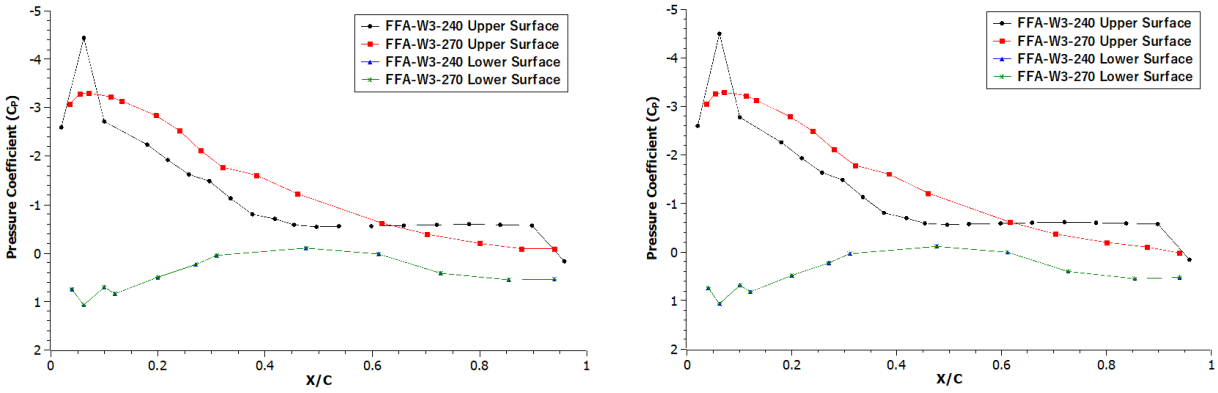

(a) Re = 0.8 × 10^6 (b) Re = 1.0 × 10^6

Figure 9: *Cp* versus *X*/*C* at angle of attack of 18°

Moreover, as indicated by Figure 7, the adverse pressure gradient begins to appear at angle of attack of 10º. When the adverse pressure gradient increases, it will cause earlier separation for thinner aerofoil but separation delay for thick aerofoil. Relative thickness affects the aerofoil performance by changing the location and size of the laminar separation bubble. In the meantime, it can be seen that increasing Reynold's number is not much affecting the pressure distribution of both aerofoil except at low angles.

Meanwhile, as shown in Figure 10 for Reynolds number of 1.0 × 10^6, stall occurs at angle of attack of 14º with maximum lift coefficient 1.26 for FFA-W3-240 aerofoil. On contrary, stall does not occur up until angle of attack of 18º for the FFA-W3-270 aerofoil with the same Reynolds number of 1.0 × 10^6 as depicted in Figure 11. Overall, both plots follow the typical trend of C_L versus angle of attack. Once the angle of attack exceeds the stalling angle, the separation occurs and the lift reduces [11]-[12]. As depicted in Figure 10, increasing the Reynold's number also increases the maximum lift coefficient for the FFA-W3-240 model. However, effect of Reynold's number is negligible for the FFA-W3-270 aerofoil as can be observed in Figure 11.

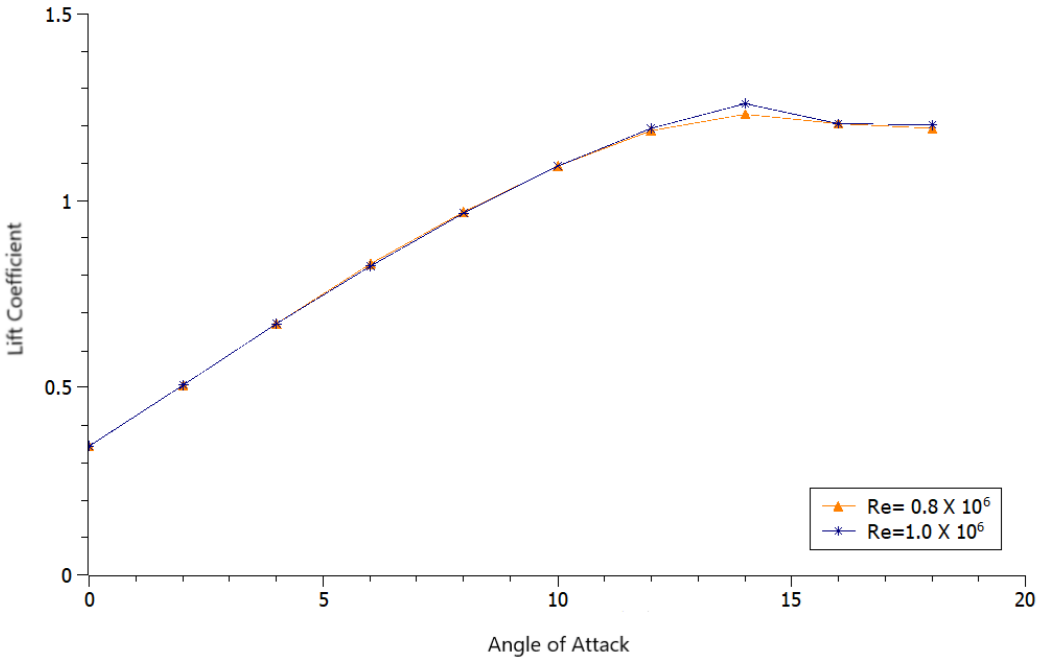

Figure 10: C_L versus angle of attack for FFA-W3-240 aerofoil

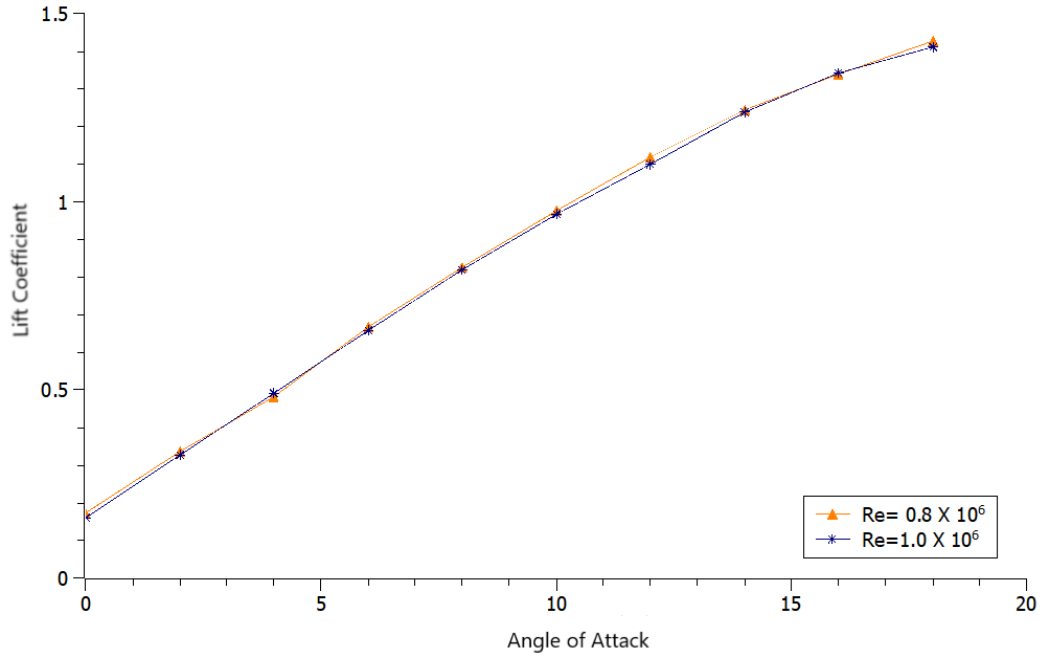

Figure 11: C_L versus angle of attack for FFA-W3-270 aerofoil

On the other hand, Figure 12 and Figure 13 depict the plot of C_D versus angle of attack for FFA-W3-240 and FFA-W3-270 aerofoil, respectively. For FFA-W3-240 aerofoil, at Reynolds number of 1.0×10^6, the drag coefficient at stall angle is shown to increase by over 5.48% compared to that at Reynolds number of 0.8×10^6. However, variation of Reynolds number has insignificant effect on drag coefficient value for the FFA-W3-270 aerofoil. The findings are in line with the results in another study, which has discovered that increasing the thickness of the aerofoil is associated with higher drag coefficient and an earlier occurrence of flow separation on the upper surface of the aerofoil [6].

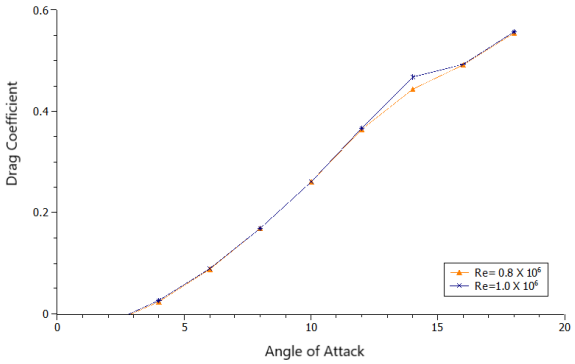

Figure 12: C_D versus angle of attack for FFA-W3-240 aerofoil

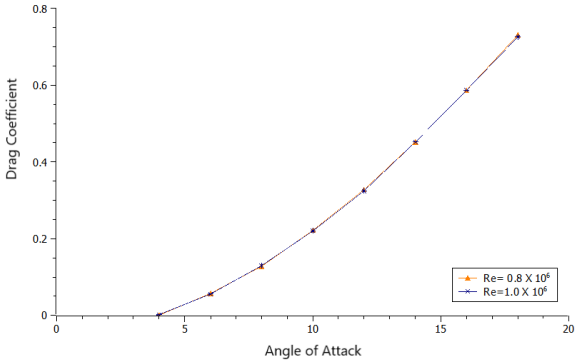

Figure 13: C_D versus angle of attack for FFA-W3-270 aerofoil

Last but not least, the resultant pitching moment coefficient of both FFA-W3-240 and FFA-W3-270 aerofoil are shown in Figure 14 and Figure 15, respectively. For FFA-W3-240 aerofoil, at Reynolds number of 1.0×10^6, the value of pitching moment coefficient at stall point is slightly higher than that at Reynolds number of 0.8×10^6. After the stall angle, the pitching moment coefficient start to decrease. This situation can be contributed to the flow separation during stall that leads to significant decrease in lift generation. Since the pitching moment coefficient is a measure of the balance between the lift forces acting on airfoil, the reduced lift after stall contributes to a decrease in the pitching moment coefficient.

Both FFA-W3-240 and FFA-W3-270 aerofoil are engineered to maintain a relatively constant pitching moment coefficient across a spectrum of angles of attack. Furthermore, since the moment coefficient is computed around the aerodynamic center point ($C/4$), influence of angle of attack is minimized [8].

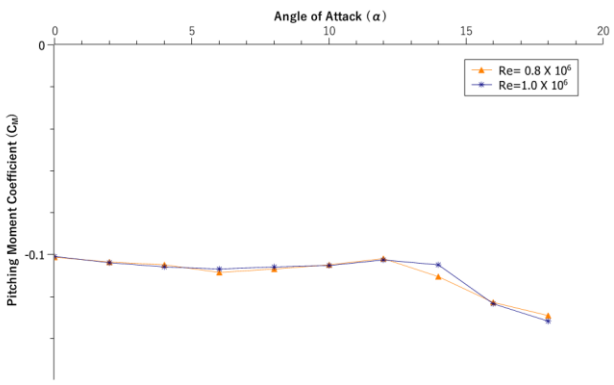

Figure 14: C_M versus angle of attack for FFA-W3-240 aerofoil

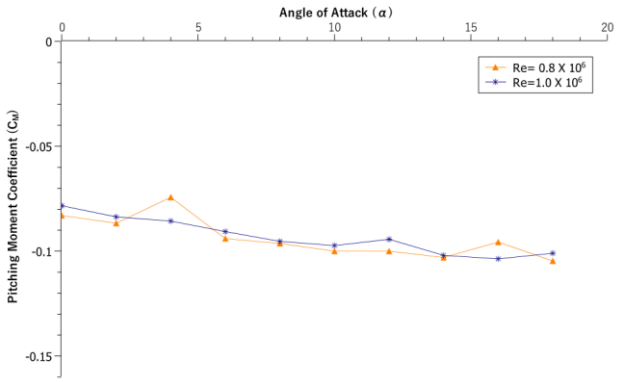

Figure 15: C_M versus angle of attack for FFA-W3-270 aerofoil

4. Conclusion

When compared to FFA-W3-270 aerofoil, it is found that pressure coefficient on the upper surface of FFA-W3-240 aerofoil has undergone a significant change. When the adverse pressure gradient grows, it causes separation to occur sooner for thinner airfoils but later for thicker airfoils. The findings from this study demonstrate that FFA-W3-270 aerofoil performs better than FFA-W3-240 aerofoil because a high performance requires the flow attachment to be maintained for as long as possible to maximize the lift generation. Regarding the lift coefficient, a higher maximum relative thickness results in a greater maximum lift. Elevating the Reynolds number boosts the maximum lift coefficient for FFA-W3-240 at Reynolds number of 1.0×10^6 with lift coefficient of 1.26 at angle of 14º. On contrary, for FFA-W3-270, stall does not occur until 18º. Increasing the Reynolds number for FFA-W3-240 amplifies the drag coefficient at the stall point by over 5.48%. For both aerofoil, the pitching moment coefficient remains relatively constant across various angles of attack. In the future works, it is advised to change the angle of attack up to 30º and alter the Reynolds number to notice more on the flow separation especially on the FFA-W3-270 aerofoil.

Acknowledgement

The authors would like to thank Aerolab UTM (Universiti Teknologi Malaysia) for the use of their facilities and everybody involved who shared their expertise and assistance. Their guidance and financial support are much appreciated.

References

[1] M. Scungio, F. Arpino, V. Focanti, M. Profili and M. Rotondi, 'Wind Tunnel Testing of Scaled Models of Newly Developed Darrieus-style Vertical Axis Wind Turbine with Auxiliary Straight Blades', Energy Conversion and Management, vol. 130, pp. 60-70, 2016.

[2] O. F. Marzuki, A. S. Mohd Rafie, F. I. Romli and K. A. Ahmad, 'Magnus Wind Turbine: The Effect of Sandpaper Surface Roughness on Cylinder Blades', Acta Mechanica, vol. 229, pp. 71-85, 2018.

[3] L. Xu, L. Xu, L. Zhang and K. Yang, 'Design of Wind Turbine Blade with Thick Airfoils and Flatback and Its Aerodynamic Characteristic', The Open Mechanical Engineering Journal, vol. 9, no. 1, pp. 910-915, 2015.

[4] A. H. Muheisen, M. A. R. Yass, I. K. Irthiea, 'Enhancement of Horizontal Wind Turbine Blade Performance using Multiple Airfoils Sections and Fences', Journal of King Saud University - Engineering Sciences, vol. 35, no. 1, pp. 69-81, 2023.

[5] A. Bjorck, 'Coordinates and Calculation for the FFA-W1-xxx, FFA-W2-xxx and FFA-W3-xxx Series of Airfoils for Horizontal Axis Wind Turbines', Report No. FFA TN 1990-15, Aeronautical Research Institute of Sweden, 1990.

[6] O. A. Abdulkareem, A. F. Khudheyer and A. S. Abbas, 'Numerical Investigation of the Effect of Changing the Thickness of Airfoils Used in Wind Turbines on the Lift to Drag Ratio', IOP Conference Series: Materials Science and Engineering, vol. 1094, no. 1, 012078, 2021.

[7] D. Ma, Y. Zhao, Y. Qiao and G. Li, 'Effects of Relative Thickness on Aerodynamic Characteristics of Airfoil at a Low Reynolds Number', Chinese Journal of Aeronautics, vol. 28, no. 4, pp. 1003–1015, 2015.

[8] S. Jafari-Gahraz, T. B. Mat Lazim, G. E. Schneider and M. Darbandi, 'Experimental Study on Aerodynamic Performance of FFA-W3-270 Airfoil for Axial Wind Turbine Blade', Presented at International Conference of Fluid Flow, Heat and Mass Transfer, Ottawa, Canada, 2016.

[9] A. V. Arena and T. J. Mueller, 'Laminar Separation, Transition and Turbulent Reattachment Near the Leading Edge of Airfoils', AIAA Journal, vol. 18, no. 7, pp. 747-753, 1980.

[10] T. Nakano, N. Fujisawa, Y. Oguma, Y. Takagi and S. Lee, 'Experimental Study on Flow and Noise Characteristics of NACA0018 Airfoil', Journal of Wind Engineering and Industrial Aerodynamics, vol. 95, no. 7, pp. 511-531, 2007.

[11] F. I. Romli, M. A. Mohammad Sabri and R. E. Mohd Nasir, 'Optimization of a Blended-Wing-Body Unmanned Aerial Vehicle Design for Maximum Aerodynamic Lift-to-Drag Ratio', CFD Letters, vol. 15, no. 3, pp. 12-21, 2023.

[12] M. Z. Abdul Manaf, S. Mat, S. Mansor, T. Mat Lazim, W. K. Wan Ali, W. Z. Wan Omar, Z. Mohd Ali, A. Abdullatif and M. Abd Wahid, 'Influences of External Store on Aerodynamic Performance of UTM-LST Generic Light Aircraft Model', Journal of Advanced Research in Fluid Mechanics and Thermal Sciences, vol. 39, no. 1, pp. 36-46, 2017.